ARTICLES

NN core interactions and differential cross sections from one gluon exchange

T. Barnes

Physics Division and Center for Computationally Intensive Physics, Oak Ridge National Laboratory,
Oak Ridge, Tennessee 37831
and Department of Physics, University of Tennessee, Knoxville, Tennessee 37996

S. Capstick

Continuous Electron Beam Accelerator Facility, 12000 Jefferson Avenue, Newport News, Virginia 23606

M. D. Kovarik

Physics Division and Center for Computationally Intensive Physics, Oak Ridge National Laboratory,
Oak Ridge, Tennessee 37831
and University of Tennessee Computer Center, University of Tennessee, Knoxville, Tennessee 37996

E. S. Swanson

Center for Theoretical Physics, Laboratory of Nuclear Science and Department of Physics,
Massachusetts Institute of Technology, Cambridge, Massachusetts 02139
(Received 17 February 1993)

We derive nonstrange baryon-baryon scattering amplitudes in the nonrelativistic quark model using the "quark Born diagram" formalism. This approach describes the scattering as a single interaction, here the one-gluon-exchange (OGE) spin-spin term followed by constituent interchange, with external nonrelativistic baryon wave functions attached to the scattering diagrams to incorporate higher-twist wave-function effects. The short-range repulsive core in the NN interaction has previously been attributed to this spin-spin interaction in the literature; we find that these perturbative constituent-interchange diagrams do indeed predict repulsive interactions in all I, S channels of the nucleon-nucleon system, and we compare our results for the equivalent short-range potentials to the core potentials found by other authors using nonperturbative methods. We also apply our perturbative techniques to the $N\Delta$ and $\Delta\Delta$ systems: Some $\Delta\Delta$ channels are found to have attractive core potentials and may accommodate "molecular" bound states near threshold. Finally we use our Born formalism to calculate the NN differential cross section, which we compare with experimental results for unpolarized proton-proton elastic scattering. We find that several familiar features of the experimental differential cross section are reproduced by our Born-order result.

PACS number(s): 21.30.+y, 24.10.−i

I. INTRODUCTION

The nucleon-nucleon interaction exhibits a strongly repulsive short-distance core and a longer-ranged but much weaker attraction. Although there has been evidence of the general features of this interaction for over 50 years [1], the physical mechanisms proposed as the origin of the interaction have changed as our understanding of the strong interaction has progressed. In 1935 Yukawa [2] suggested that the finite-ranged nuclear attraction was due to the exchange of a massive, strongly interacting meson, by analogy with electron sharing as the origin of chemical forces. This hypothetical meson was identified with the pion after its discovery, and as the lightest hadron it certainly contributes the longest-ranged component of the nucleon-nucleon strong force. The repulsive short-range core of the nucleon-nucleon interac-

tion was similarly attributed to the exchange of heavier mesons such as the ω after their discovery. These meson-exchange models have been elaborated considerably since these original suggestions, and the most accurate phenomenological descriptions of the nucleon-nucleon interaction at present are meson-exchange models [3], with parameters such as meson-nucleon couplings fitted to experiment.

A literal attribution of the short-range repulsive core to vector meson exchange, as opposed to a phenomenological parametrization, of course involves a *nonsequitur* [4, 5]: Since the nucleons have radii of ≈ 0.8 fm, and the range of the vector-exchange force is $1/m_\omega \approx 0.2$ fm, one would have to superimpose the nucleon wave functions to reach the appropriate internucleon separations. The picture of distinct nucleons exchanging a physical ω meson at such a small separation is clearly a fiction, and

a realistic description of the short-range core interaction requires a treatment of the quark wave functions of the interacting nucleons and a Hamiltonian which involves quark and gluon degrees of freedom.

Since the development of QCD as the theory of the strong interaction, there have been many studies of the NN interaction in terms of quarks and gluons. Most have employed the nonrelativistic quark potential model, although some early work used the MIT bag model [6]. Many studies of this and other multiquark systems were fundamentally flawed due to an inadequate treatment of the color degree of freedom, or due to assumptions that imposed confinement on the entire multiquark system; a discussion of these problems is given by Isgur [4]. It now appears that a pairwise $\lambda \cdot \lambda$ color interaction [7–9] together with a sufficiently general spatial wave function that allows dissociation into color singlets provides a sufficiently realistic description of color forces in a multiquark system. The NN references summarized here all assume the $\lambda \cdot \lambda$ form, and it has also become standard to employ a quadratic or linear confinement potential. Finally, the spin-spin hyperfine term is incorporated in all these references, as it apparently makes a dominant contribution to the NN core interaction. Several groups have included other terms from the Breit-Fermi interaction such as the hyperfine-tensor and spin-orbit interactions.

Attempts to describe the NN interaction using quark potential models date from the work of Liberman in 1977 [10], who calculated the adiabatic response of the six quark system to variations in the interbaryon coordinate. The resulting effective potential had a repulsive core with a weak intermediate-range attraction. Liberman concluded that the repulsive core was predominantly due to a combination of the Pauli principle and the contact hyperfine term. The same conclusion was reached by Neudatchin and collaborators [11], also within the adiabatic approximation. Harvey [12] continued this adiabatic approach in a generalized calculation of the effective NN potential; he noted that SU(4) spin-isospin symmetry required that NN, $\Delta\Delta$, and "hidden color" $(qqq)_8 \otimes (qqq)_8$ states be included in the calculation. On incorporating these states, he found that the repulsive core was strongly suppressed. It is now widely believed that the absence of the repulsive core in improved calculations is an artifact of the adiabatic approximation [13, 14].

The usual method for improving on the adiabatic approximation in the q^6 system is to employ the resonating-group method. This involves expanding the wave function of the system in a basis which describes system subclusters multiplied by unknown functions of the intercluster coordinates. One then solves the resulting coupled integro-differential equations using various numerical techniques. Baryon subcluster wave functions are usually taken to be simple Gaussians, and the coupled system is truncated at the NN, $NN + \Delta\Delta$, or $NN + \Delta\Delta +$ hidden color levels. The first applications of the resonating-group method to the NN system were given by Warke and Shanker [15], Oka and Yazaki [16], and Ribeiro [17]. All groups found a repulsive core, which was dominantly due to the Pauli principle and the color

hyperfine term. The $\Delta\Delta$ and hidden color channels were found to make only small contributions to the hardcore S-wave phase shifts. These studies found that several contributions including the Coulomb and confinement kernels approximately canceled, leaving the spin-spin OGE hyperfine term as the dominant interaction. The resonating-group approach has been extended to include more channels, strange quarks, effective one-boson-exchange long-range potentials, and virtual excitations of the quark wave functions. In particular, Koike [18] has applied these techniques to the "flip-flop" model [19] (which eliminates long-range color van der Waals forces), supplemented by an effective meson-exchange potential, and Cao and Kisslinger [20] have developed a relativistic resonating-group formalism and applied it to the determination of equivalent potentials and low-L phase shifts in a model which incorporates OGE and meson-exchange forces. Both these references find reasonably good agreement with experimental low-energy NN phase shifts. A summary of work in this field to 1989 has been given by Shimizu [21].

Maltman and Isgur [22] have performed a detailed variational calculation of the ground-state properties of the deuteron using a $\lambda \cdot \lambda$ quark-quark interaction with the full OGE color Breit-Fermi interaction, a quadratic confinement term, and a phenomenological one-pion-exchange potential. In contrast to typical resonating-group calculations, they allowed spatial excitations within the clusters. They found a repulsive core, and noted that the admixture of P-wave color octet clusters significantly increased the range and depth of the intermediate-range attraction. Their results for the deuteron binding energy, rms radius, quadrupole moment, and magnetic moment all agreed well with experiment. Further work on the NN and $\Delta\Delta$ systems may be found in Ref. [23].

Although the origin of the short-range nucleon-nucleon force is now reasonably well understood at the QCD level, the resonating-group and variational techniques which have been employed in this work are rather intricate and require considerable theoretical effort, and lead to numerical rather than analytical results. As these techniques are best suited to the determination of ground-state properties, topics such as resonance production and scattering cross sections at higher energies have received little attention in these quark model studies.

In recent work we have investigated the possibility that these low-energy nonresonant hadronic scattering amplitudes may actually be dominated by simple perturbative processes; if so, it may be possible to derive useful estimates of these amplitudes using a much simpler approach. A complementary possibility of perturbative dominance of hadronic scattering processes at high energies through constituent-interchange mechanisms has been investigated by theorists almost since the development of QCD [24]. Results for elastic hadron-hadron scattering amplitudes, in particular the asymptotic Q^2 dependence of fixed-angle scattering, have recently been presented by Botts and Sterman [25].

Concerns regarding the range of validity of the high-energy perturbative QCD studies have been expressed

by Isgur and Llewellyn Smith [26], who suggest that higher-twist hadron wave-function effects may actually dominate perturbative QCD contributions at experimentally accessible energies. We have explicitly incorporated these wave-function effects in our study of a constituent-interchange scattering mechanism in the nonrelativistic quark potential model. We calculate the hadron-hadron scattering amplitudes which follow from one gluon exchange followed by constituent interchange (CI) (quark line interchange is required at lowest order in α_s to restore color singlet final states), with nonrelativistic quark model wave functions attached to the external lines. This OGE+CI mechanism may be dominant in processes in which $q\bar{q}$ annihilation is forbidden for the valence wave functions. We have applied this description of scattering to elastic $I = 2$ $\pi\pi$ [27] and $I = \frac{3}{2}$ $K\pi$ [28] reactions and found excellent agreement with the experimental S-wave phase shifts given standard quark model parameters.

Related approaches to calculating meson-meson scattering amplitudes which iterate this quark-gluon mechanism have been discussed in the literature [29]. These Born-order techniques have also been applied to vector-vector meson systems [30], and lead to interesting predictions of vector-vector molecule bound states in certain channels [31]. In the vector-vector system the hyperfine interaction apparently does not dominate the scattering amplitude, unlike the pseudoscalar-pseudoscalar and NN systems. More recently we applied the quark Born formalism to KN scattering [32], which is also free of $q\bar{q}$ annihilation at the valence quark level. We found satisfactory agreement with the experimental S-wave KN scattering lengths, although $I = 0$ is not yet very well determined experimentally. The KN S-wave phase shifts at higher energies, however, are not well described; they require stronger high-momentum components in the nucleon wave function than are present in the single Gaussian forms we assumed. The higher-L KN partial waves, especially the P waves, show evidence of a spin-orbit interaction which does not arise in single-channel spin-spin scattering, which has not yet been adequately explained in the literature.

The next level of complexity in Hilbert space is the q^6 baryon-baryon sector. Since this system is free of annihilation at the valence level, and the spin-spin hyperfine term has already been established as the dominant interaction underlying the core repulsion, derivation of the NN core interaction is an important test of the quark Born formalism. Here we derive the nucleon-nucleon interaction predicted by the OGE spin-spin term using quark Born diagrams, and show that the predicted core interaction is indeed strongly repulsive in all four spin and isospin channels. Low energy Born-equivalent NN core potentials are also derived and compared to previous results. We then consider other nonstrange baryons and derive the $N\Delta$ and $\Delta\Delta$ short-range interactions; some of these are found to be attractive, and we investigate the possibility that these channels might support dibaryon molecule bound states. Some of our results for attractive $\Delta\Delta$ channels are consistent with the previous conclusions of Maltman [33]. Finally we derive the elastic NN differential cross section predicted by our quark Born for-

malism and find that some familiar experimental features of the high-energy elastic proton-proton differential cross section are evident in our results.

II. DERIVATION OF SCATTERING AMPLITUDES

The method we employ involves calculating the amplitude for a given process using a Born approximation to the resonating-group equation, converting this into an effective potential, and integrating the effective Schrödinger equation to obtain nonperturbative predictions. There are several advantages to adopting this approach. One is its simplicity: Integrating a multichannel resonating-group system involves considerable effort, whereas we need only evaluate the individual entries in the effective potential matrix and then numerically integrate the simpler Schrödinger system. Furthermore, the method can provide analytic expressions for Born-order differential cross sections, scattering lengths, and other observables.

The validity of the method requires that information on the dominant physics be contained in the Born amplitudes. This is expected to be the case for reactions which do not involve meson exchange at low energy and do not allow significant quark annihilation. A comparison of the hadronic scattering amplitudes obtained from the conventional single channel resonating-group method and from integrating effective potentials (as is done here) has been made for several cases in Ref. [30] and the agreement is remarkably good.

A. Hamiltonian and hadron states

The scattering amplitude is defined by factoring out the overall momentum conserving delta function

$$_f\langle BB'|H_{\text{scat}}|BB'\rangle_i \equiv h_{fi}\, \delta(\mathbf{P}_f - \mathbf{P}_i) \ . \tag{1}$$

Since the hadron state normalizations we will introduce are identical to those used in our previous study of $I = 2$ $\pi\pi$ scattering [27], we can use the relations between the scattering matrix element h_{fi} and the phase shifts and cross sections given there. The details of our diagrammatic procedure for determining h_{fi} are described elsewhere [27, 28, 32]. For baryon-baryon scattering we shall follow previous studies [4, 10–19, 21, 22] and assume that the dominant part of the core interaction derives from the spin-spin color hyperfine term,

$$H_{\text{scat}} = \sum_{a,i<j} \left[-\frac{8\pi\alpha_s}{3m_i m_j}\, \delta(\mathbf{r}_{ij}) \right] \left[\mathbf{S}_i \cdot \mathbf{S}_j \right] \left[\mathcal{F}_i^a \cdot \mathcal{F}_j^a \right], \tag{2}$$

where $\mathcal{F}_i^a$ is the color matrix $\lambda^a/2$ for quark i. The baryon color wave functions are the usual color singlets,

$$|\text{baryon}\rangle = \sum_{i,j,k=1,3} \frac{1}{\sqrt{6}}\, \epsilon_{ijk}\, |ijk\rangle \ . \tag{3}$$

Our spin-flavor states for the meson and baryon are the usual SU(6) states, but as explained in Ref. [32] we find

it convenient to write these states using field theory conventions rather than in the usual quark model form. The quark model conventions show explicit exchange symmetry by assigning a fixed location in the state vector to each quark. The field theoretic convention greatly reduces the number of terms encountered in our scattering matrix elements; for example, the proton state in field theory conventions has only 2 terms instead of the usual 9 for quark model states, so $PP \to PP$ elastic scattering involves only 16 terms, far fewer than the 6561 we would encounter with the usual quark model conventions. As examples, the orthonormal $S_z = \frac{3}{2} \, |\Delta^+_{3/2}\rangle$ and $S_z = \frac{1}{2}$ $|P_{1/2}\rangle$ states in field theory conventions are

$$|\Delta^+_{3/2}\rangle = \frac{1}{\sqrt{2}} |u_+ u_+ d_+\rangle \tag{4}$$

and

$$|P_{1/2}\rangle = \sqrt{\frac{2}{3}} \left\{ \frac{|u_+ u_+ d_-\rangle}{\sqrt{2}} \right\} - \sqrt{\frac{1}{3}} \, |u_+ u_- d_+\rangle \, . \tag{5}$$

The other baryon states considered in this paper can be derived from these by application of spin and isospin raising and lowering operators.
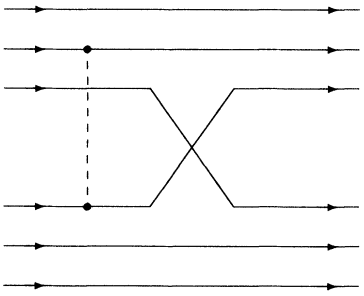
We shall quote general results for baryon-baryon scattering amplitudes with arbitrary spatial wave functions attached to the external lines and then specialize to single Gaussian forms to derive representative closed-form results. The general spatial baryon wave function we assume is of the form

$$\Phi_{\text{baryon}}(\mathbf{p}_1, \mathbf{p}_2, \mathbf{p}_3; \mathbf{P}_{\text{tot}})$$

$$= \phi_{\text{baryon}}(\mathbf{p}_1, \mathbf{p}_2, \mathbf{p}_3) \, \delta(\mathbf{P}_{\text{tot}} - \mathbf{p}_1 - \mathbf{p}_2 - \mathbf{p}_3) \tag{6}$$
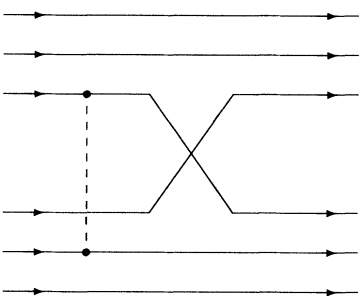
with a normalization given by

$$\langle \Phi_{\text{baryon}}(\mathbf{P}'_{\text{tot}}) | \Phi_{\text{baryon}}(\mathbf{P}_{\text{tot}}) \rangle$$

$$= \int\!\!\int\!\!\int\!\!\int\!\!\int\!\!\int d\mathbf{p}_1 \, d\mathbf{p}_2 \, d\mathbf{p}_3 \, d\mathbf{p}_1{}' \, \mathbf{p}_2{}' \, d\mathbf{p}_3{}' \, \Phi^*_{\text{baryon}}(\mathbf{p}_1{}', \mathbf{p}_2{}', \mathbf{p}_3{}'; \mathbf{P}'_{\text{tot}}) \Phi_{\text{baryon}}(\mathbf{p}_1, \mathbf{p}_2, \mathbf{p}_3; \mathbf{P}_{\text{tot}})$$

$$= \delta(\mathbf{P}_{\text{tot}} - \mathbf{P}'_{\text{tot}}) \, . \tag{7}$$

The standard quark model single Gaussian baryon wave function we shall use for illustration is

$$\phi_{\text{baryon}}(\mathbf{p}_1, \mathbf{p}_2, \mathbf{p}_3) = \frac{3^{3/4}}{\pi^{3/2}\alpha^3} \exp\left\{ -\frac{(\mathbf{p}_1^2 + \mathbf{p}_2^2 + \mathbf{p}_3^2 - \mathbf{p}_1 \cdot \mathbf{p}_2 - \mathbf{p}_2 \cdot \mathbf{p}_3 - \mathbf{p}_3 \cdot \mathbf{p}_1)}{3\alpha^2} \right\} \, . \tag{8}$$

Oscillator parameter values of $0.25 \text{ GeV} \leq \alpha \leq 0.42 \text{ GeV}$ have been used in the quark model literature on baryon spectroscopy, as we will discuss subsequently.

B. Baryon-baryon scattering amplitudes

By analogy with our study of KN scattering [32] (see especially Sec. II B) we first write a generic scattering diagram with initial and final baryon-baryon states. We then connect the initial and final quark lines in all ways consistent with flavor conservation; for example, $\Delta^{++}\Delta^{++}$ elastic scattering has 6!=720 quark line diagrams. These may be grouped into four sets in which

the number of $q\bar{q}$ pairs which cross in the t channel is 0,1,2, or 3. We then generate scattering diagrams by inserting one-gluon-exchange interactions between all pairs of initial quarks in different initial baryons; this gives nine times as many scattering diagrams as we had quark line diagrams. Many of these diagrams are trivially zero; these include the zero-pair-interchange and three-pair-interchange diagrams, which vanish due to color. The nonzero scattering diagrams may be related to a small "reduced set" of diagrams by permutation of external lines, which leaves a diagram invariant. In baryon-baryon scattering this reduced set contains eight independent diagrams, which are shown below:
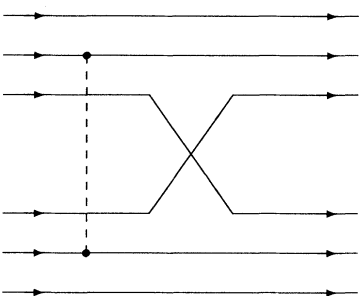

$$D_1 \quad = \qquad\qquad\qquad\qquad\qquad\qquad\qquad\qquad \tag{9}$$
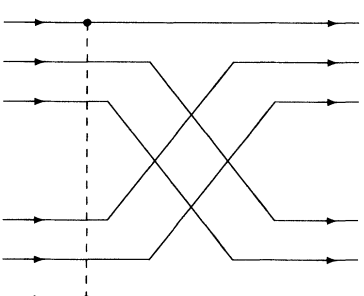
$$D_2 \quad = \quad \text{(10)}$$
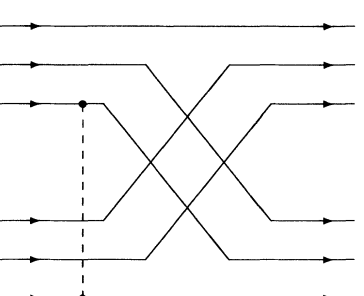
$$D_3 \quad = \quad \text{(11)}$$

$$D_4 \quad = \quad \text{(12)}$$

$$D_5 \quad = \quad \text{(13)}$$

$$D_6 \quad = \quad \text{(14)}$$

$$D_7 \quad = \qquad\qquad\qquad\qquad\qquad\qquad\qquad\qquad\qquad\qquad\qquad (15)$$

,

$$D_8 \quad = \qquad\qquad\qquad\qquad\qquad\qquad\qquad\qquad\qquad\qquad\qquad (16)$$

.

In a given baryon-baryon scattering process the matrix element h_{fi} in (1) is a weighted sum of the eight spatial overlap integrals represented by the diagrams $D_1 \cdots D_8$,

$$h_{fi} = \sum_{n=1}^{8} w_n I_n(D_n) . \qquad (17)$$

The weight of each diagram (introduced in [32]) is the product of a color factor, a fermion permutation phase called the "signature" of the diagram (which is -1 for $D_1 \cdots D_4$ and $+1$ for $D_5 \cdots D_8$), the overall $(-)$ in H_I (2), and a reaction-dependent spin-flavor factor. The derivation of these factors and the spatial overlap integrals they multiply is discussed in detail elsewhere [27, 32], so here we will simply present results with minimal discussion. There is a minor change in the convention for diagram weights relative to our earlier reference. In our KN study [32] we incorporated the $(-)$ phase of H_I and the signature phase in the spatial overlap integral; here we include them in the diagram weight. This overall factor was $(+1)$ for all KN diagrams, so the KN weights are unchanged by our new convention. Similarly, in our first paper [27] we incorporated the $(-)$ phase of H_I in the spatial overlap integral. Our new convention is useful because it makes all the NN spatial overlap integrals considered here positive, so the overall amplitude phases are clear from the weights alone.

The color factors of the diagrams $D_1 \cdots D_8$ are

$$I_{\text{color}}([D_1 \cdots D_8])$$

$$= \left[+\tfrac{4}{9}, -\tfrac{2}{9}, -\tfrac{2}{9}, +\tfrac{1}{9}, +\tfrac{4}{9}, -\tfrac{2}{9}, -\tfrac{2}{9}, +\tfrac{1}{9} \right] . \quad (18)$$

D_n is related to D_{n+4} by $t \leftrightarrow u$ crossing; for this reason the weights w_n and w_{n+4} are closely related in many reactions. To simplify our presentation, when possible

we will just give results for the weights of $D_1 \cdots D_4$ and indicate the relative phase of the set for $D_5 \cdots D_8$ after a vertical bar. Thus for $\{I_{\text{color}}(D_n)\}$ above we write

$$I_{\text{color}} = \left[+\tfrac{4}{9}, -\tfrac{2}{9}, -\tfrac{2}{9}, +\tfrac{1}{9} \,\middle|\, (+) \right] . \quad (19)$$

The spin-flavor weights (incorporating the signature phases) are just matrix elements of the operator $\mathbf{S}_i \cdot \mathbf{S}_j$ between two initial quarks for the given process. As an example, for $\Delta^{++}\Delta^{++}$, $S = 3, S_z = 3$ scattering there are four $|u_+ u_+ u_+\rangle/\sqrt{6}$ external baryons, and only the $S_i^z S_j^z$ terms contribute. On summing over all scattering diagrams in this channel we find

$$I_{\text{spin-flavor}} I_{\text{signature}} \Big|_{\Delta\Delta, I=3, S=3}$$

$$= \left[+\tfrac{9}{4}, +\tfrac{9}{2}, +\tfrac{9}{2}, +9 \,\middle|\, (-) \right] , \quad (20)$$

which is I_z and S_z independent. Combining these we find the $I = 3, S = 3$ $\Delta\Delta$ diagram weights,

$$\{w_n(\Delta\Delta, \ I = 3, S = 3)\} = \left[+1, -1, -1, +1 \,\middle|\, (-) \right] . \quad (21)$$

Since the spatial overlap integrals $I_5(D_5) \cdots I_8(D_8)$ are equal to the integrals $I_1(D_1) \cdots I_4(D_4)$ after $t \leftrightarrow u$ crossing, the relative $(-)$ phase in the diagram weights (21) ensures that the $I = 3, S = 3$ $\Delta\Delta$ scattering amplitude h_{fi} is spatially antisymmetric, as required for a totally antisymmetric fermion-fermion scattering amplitude that is symmetric in the remaining degrees of freedom (I and S). This antisymmetry is a nontrivial check of our spin-flavor combinatorics, since it is only evident after the sum over individual quark-gluon scattering diagrams is completed.

The diagram weights for all I, S channels of NN, $N\Delta$, and $\Delta\Delta$ elastic scattering are tabulated at the end of the paper; these and the overlap integrals constitute our central results.

The spatial overlap integrals associated with the diagrams may be determined using the simple diagrammatic techniques presented in Appendix C of Ref. [27]. In these integrals all momenta are implicitly three dimensional,

and have an overall spin-spin coefficient κ_{ss} of

$$\kappa_{ss} = \frac{8\pi\alpha_s}{3m_q^2}\frac{1}{(2\pi)^3} \ . \tag{22}$$

This is (-1) times the κ of [27], since we have chosen to include the $(-)$ phase of H_I (2) in the diagram weight factor, as discussed above. The integrals are

$$I_1 = \kappa_{ss}\iint da_1 da_2\ \Phi_A(a_1, a_2, A - a_1 - a_2)\Phi_C^*(a_1, a_2, C - a_1 - a_2)$$

$$\times \iint db_2 db_3\ \Phi_B(-A - b_2 - b_3, b_2, b_3)\Phi_D^*(-C - b_2 - b_3, b_2, b_3)\ ; \tag{23}$$

$$I_2 = \kappa_{ss}\iiiint da_1 da_3 db_2 dc_3\ \Phi_A(a_1, A - a_1 - a_3, a_3)\Phi_C^*(a_1, C - a_1 - c_3, c_3)$$

$$\times \Phi_B(C - A + a_3, b_2, -C - a_3 - b_2)\Phi_D^*(a_3, b_2, -C - a_3 - b_2)\ , \tag{24}$$

$$I_3 = \kappa_{ss}\iiiint da_1 da_2 db_3 dd_1\ \Phi_A(a_1, a_2, A - a_1 - a_2)\Phi_C^*(a_1, a_2, C - a_1 - a_2)$$

$$\times \Phi_B(C - a_1 - a_2, -A - C + a_1 + a_2 - b_3, b_3)\Phi_D^*(d_1, -C - b_3 - d_1, b_3)\ , \tag{25}$$

$$I_4 = \kappa_{ss}\iiiint da_1 da_3 db_1 db_3\ \Phi_A(a_1, A - a_1 - a_3, a_3)\Phi_C^*(a_1, C - a_1 - b_1, b_1)$$

$$\times \Phi_B(b_1, -A - b_1 - b_3, b_3)\Phi_D^*(a_3, -C - a_3 - b_3, b_3)\ . \tag{26}$$

We evaluate these in the c.m. frame, so the $t \leftrightarrow u$ crossed integrals $I_5 \cdots I_8$ can be obtained by exchanging $\mathbf{C}$ and $\mathbf{D} = -\mathbf{C}$, or in terms of the cosine of the c.m. scattering angle $\mu = \cos(\theta_{\text{c.m.}})$,

$$I_{n+4}(\mu) = I_n(-\mu)\ . \tag{27}$$

A simplification follows if all baryons have the same spatial wave functions, as we assume here; in this case $I_2 = I_3$ and hence $I_6 = I_7$.

The overlap integrals may be carried out in closed form given single Gaussian wave functions (8), and each gives a result of the form

$$I_n = \kappa_{ss}\,\eta_n\,\exp\left\{-(A_n - B_n\mu)P^2\right\}\ , \tag{28}$$

where P is the magnitude of the c.m. three-momentum of each baryon, $P^2 = \mathbf{A}^2 = \mathbf{B}^2 = \mathbf{C}^2 = \mathbf{D}^2$. The results are

$$I_1 = \kappa_{ss}\exp\left\{-\frac{1}{3\alpha^2}(\mathbf{A} - \mathbf{C})^2\right\}$$

$$= \kappa_{ss}\exp\left\{-\frac{1}{3\alpha^2}2(1 - \mu)P^2\right\}$$

$$= \kappa_{ss}\exp\left\{\frac{t}{3\alpha^2}\right\}\ , \tag{29}$$

$$I_2 = I_3$$

$$= \kappa_{ss}\left(\frac{12}{11}\right)^{3/2}\exp\left\{-\frac{1}{33\alpha^2}(20 - 12\mu)P^2\right\}$$

$$= \kappa_{ss}\left(\frac{12}{11}\right)^{3/2}\exp\left\{-\frac{2(s - 4M^2)}{33\alpha^2}\right\}\exp\left\{\frac{2t}{11\alpha^2}\right\}\ , \tag{30}$$

$$I_4 = \kappa_{ss}\left(\frac{3}{4}\right)^{3/2}\exp\left\{-\frac{1}{3\alpha^2}P^2\right\}$$

$$= \kappa_{ss}\left(\frac{3}{4}\right)^{3/2}\exp\left\{-\frac{(s - 4M^2)}{12\alpha^2}\right\}\ . \tag{31}$$

In the final expression for each integral we have substituted for P^2 and μ in terms of the Mandelstam variables s and t using relativistic kinematics, $s = 4(P^2 + M^2)$ and $t = -2(1 - \mu)P^2$.

Near threshold the overlap integrals are comparable in magnitude, but at higher energies their behaviors differ markedly. All but I_1 and its crossing-symmetric partner I_5 are strongly suppressed in s; diagrams D_1 and D_5 therefore dominate at high energies, for forward and backward scatterings, respectively. This behavior is due to the mechanism of "minimum spectator suppression," as was discussed in detail in Sec. II E of Ref. [32]. To summarize the arguments for this case: (1) for for-

TABLE I.   Diagram weights for NN elastic scattering.

	ω_1	ω_2	ω_3	ω_4	Rel. phase $\omega_5 \cdots \omega_8$
$I = 1$, $S=1$	$\frac{59}{81}$	$\frac{17}{81}$	$\frac{17}{81}$	$\frac{10}{81}$	$(-)$
$S=0$	$\frac{31}{27}$	$\frac{7}{27}$	$\frac{7}{27}$	0	$(+)$
$I=0$, $S=1$	$\frac{19}{27}$	$\frac{7}{27}$	$\frac{7}{27}$	$\frac{2}{27}$	$(+)$
$S=0$	$-\frac{1}{9}$	$\frac{5}{9}$	$\frac{5}{9}$	0	$(-)$

ward scatterings, $\mathbf{A} = \mathbf{C}$, diagram D_1 (9) requires no spectator to cross into an opposite-momentum hadron, which would carry considerable suppression due to a small wave-function overlap; only the hard-scattered constituents are required to reverse momentum. (2) D_5 (13) requires all spectators that were initially in a baryon with momentum $\mathbf{A}$ to reside finally in a baryon with momentum $\mathbf{D}$. Clearly the suppression due to wave-function overlaps of the spectators will be less important if the final baryon D has the same momentum as the initial baryon A, $\mathbf{D} = \mathbf{A}$. This corresponds to backscatter, $\mathbf{C} = -\mathbf{A}$, since $\mathbf{C} = -\mathbf{D}$ in the c.m. frame. As in D_1, only the hard-scattered quarks are then required to recoil into a baryon with three-momentum opposite to that of their initial baryon. These two explanations are actually equivalent because D_1 and D_5 are related by crossing.

III. NN CORE POTENTIALS AND PHASE SHIFTS

The Hamiltonian matrix elements

$$h_{fi} = \sum_{n=1}^{8} w_n I_n \tag{32}$$

for the four I, S channels accessible in NN scattering are summarized by the diagram weights in Table I. Specializing to the even-L channels $I, S=0,1$ and $1,0$, for which a repulsive core in S wave is a well-known feature, we see that all eight coefficients $\{w_1 \cdots w_8\}$ are positive or zero in both cases, corresponding to a repulsive interaction. For a more quantitative evaluation we can relate this h_{fi} matrix element to an NN potential near threshold, which is defined to give the same low-energy scattering amplitude near threshold in Born approximation. (See Appendix E of Ref. [27] for a detailed discussion.) For an h_{fi} of the form

$$h_{fi} = \frac{8\pi\alpha_s}{3m_q^2} \frac{1}{(2\pi)^3} \sum_{n=1}^{4} w_n \eta_n \exp\left\{ -(A_n - B_n\mu)P^2 \right\} \tag{33}$$

the Born-equivalent potential is

$$V_{NN}(r)$$

$$= \frac{8\alpha_s}{3\sqrt{\pi}m_q^2} \sum_{n=1}^{4} \frac{w_n \eta_n}{(A_n + B_n)^{3/2}} \exp\left\{ -\frac{r^2}{(A_n + B_n)} \right\} . \tag{34}$$

The $t \leftrightarrow u$ crossed diagrams $D_5 \cdots D_8$ are not included in this sum because they will automatically be generated by the crossed diagram in $NN \rightarrow NN$ potential scattering through $V_{NN}(r)$.

The numerical potentials predicted for S-wave $I = 0$ and $I = 1$ NN systems are shown in Fig. 1 for our "reference" set of quark model parameters [32], $\alpha_s = 0.6$, $m_q = 0.33$ GeV, and $\alpha = 0.4$ GeV. A discussion of the parameters used in previous work is given in the Appendix. Actually only the two parameters $\alpha_s/m_q^2 = 5.51$ GeV^{-2} and $\alpha = 0.4$ GeV are involved in our $V_{NN}(r)$. These potentials are consistent with expectations for NN core interactions; they are repulsive and have ranges of about $\frac{1}{2}$ fm and peak values comparable to $+1$ GeV, which is essentially infinite from a nuclear physics viewpoint. It may be interesting in future work to parametrize the amplitudes associated with each diagram (the weights in Table I) as a two-nucleon spin and isospin interaction of the form $A\,I + B\,\mathbf{S}_1 \cdot \mathbf{S}_2 + C\,\boldsymbol{\tau}_1 \cdot \boldsymbol{\tau}_2 + D\,\mathbf{S}_1 \cdot \mathbf{S}_2\,\boldsymbol{\tau}_1 \cdot \boldsymbol{\tau}_2$, which will allow a more direct comparison with meson-exchange models [34].

Low-energy equivalent NN core potentials have been presented as the results of some of the NN resonating-group and variational calculations we discussed in the Introduction. In their Figs. 1 and 2 Suzuki and Hecht [35] show numerical results for the NN core potentials of Harvey [12], Faessler, Fernandez, Lübeck, and Shimizu [13], and Oka and Yazaki [16]. The Faessler et al. and Oka-Yazaki potentials are quite similar to our potentials in Fig. 1, with values at the origin between 0.6 and 1.0
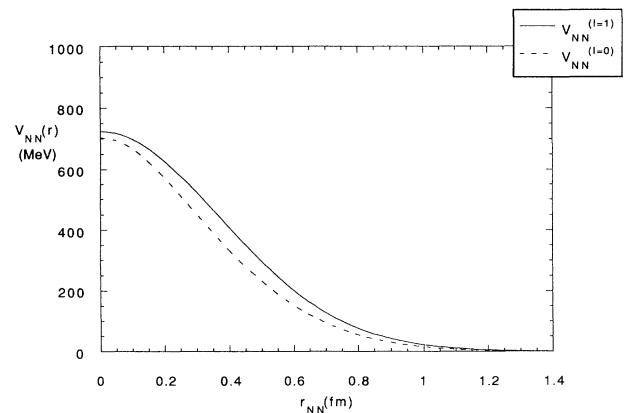

FIG. 1. NN core potentials from quark Born diagrams. Parameter set $\alpha_s/m_q^2 = 0.6/(0.33)^2$ GeV^{-2} and $\alpha = 0.4$ GeV.

GeV and comparable ranges. Harvey finds potentials with somewhat longer ranges, which Suzuki and Hecht attribute to his choice of a larger nucleon width parameter, $b_N \equiv 1/\alpha = 0.8$ fm; the Faessler *et al.* and Oka-Yazaki values are 0.475 fm and 0.6 fm, respectively, and we use a comparable $1/\alpha = 0.493$ fm.

The *NN* core potentials found by Maltman and Isgur, in Fig. 1 of Ref. [22], also have similar ranges but are somewhat larger in magnitude, $V(0)$=1.2 GeV for $I = 0$ and 2.3 GeV for $I = 1$. Our difference in the contact values is due in part to the choice of parameters; in our calculations the potentials are proportional to $\alpha_s \alpha^3/m_q^2$, which is 0.353 GeV with our parameters and 0.489 GeV for Maltman and Isgur (see the Appendix). Note, however, that no other reference finds the large Maltman-Isgur $I = 1/I = 0$ ratio at contact. The value chosen for $\alpha_s \alpha^3/m_q^2$ by itself does not explain the differences between potentials; those reviewed by Suzuki and Hecht use $\alpha_s \alpha^3/m_q^2 \approx 0.55$ GeV, so we would naively expect our potentials to be ≈ 0.6 times as large as theirs. Of course the values near the origin have little physical relevance due to their small Jacobean weight, and in any case we are comparing potentials derived using three different methods which may preclude a more accurate comparison of results.

Note in Fig. 1 that the intermediate-range attractions which are responsible for the deuteron in $I = 0$ and its almost-bound $I = 1$ partner are absent from our quark Born potentials. This is as we anticipated, given that these attractions arise mainly from a spatial distortion of interacting-nucleon wave functions [4, 22]; in our leading-order Born calculation we assume fixed nucleon spatial wave functions. The attraction presumably arises at higher order in the Born series, and may be accessible through leading-order Born calculations of off-diagonal matrix elements.

Oka and Yazaki (Fig. 2 of [16]) and Koike (Fig. 3 of [18]) also show the *S*-wave phase shifts which result from their *NN* core interactions. In Fig. 2 we show the *S*-wave phase shifts we find on numerically integrating the Schrödinger equation with the potentials of Fig. 1. Our phase shifts are very similar to the results of these earlier resonating-group studies. Although we would like to compare our phase shifts to experiment directly, the experimental phase shifts [36] are unfortunately complicated by the presence of the deuteron and its $I = 1$ partner near threshold. These states will have to be incorporated in our calculation before we can make a useful comparison between our theoretical core phase shifts and experiment.

The Born-order approximate phase shifts (proportional to h_{fi}) can be determined analytically using Eq. (6) of [28] and dividing by 2 for identical particles,

$$\delta^{(\ell)} = -\frac{\pi^2}{2}PE_P \int_{-1}^{1} h_{fi}(\mu)P_\ell(\mu). \qquad (35)$$

The momentum, energy, and $\mu = \cos(\theta_{\text{c.m.}})$ are for one nucleon in the c.m. frame. From our general result for h_{fi} (17) and the Gaussian wave-function integrals (28), we find an ℓth Born-order partial-wave phase shift of

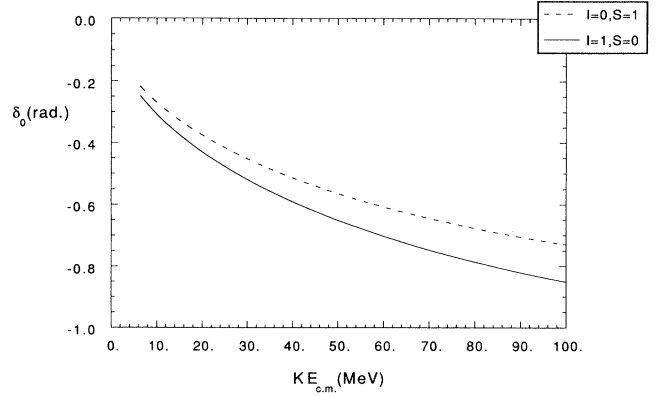
FIG. 2. *NN* core *S*-wave phase shifts from the quark Born $V_{NN}(r)$. Parameter set $\alpha_s/m_q^2 = 0.6/(0.33)^2$ GeV^{-2} and $\alpha = 0.4$ GeV.

$$\delta^{(\ell)} = -\frac{\alpha_s}{3m_q^2}PE_P \sum_{n=1}^{8} w_n \eta_n e^{-A_n P^2} i_\ell(B_n P^2) . \qquad (36)$$

The spin dependence of this result is implicit in the weights $\{w_n\}$. Note that these phase shifts are functions of ℓ and spins only, so there is no spin-orbit force in our effective *NN* interaction. This is as expected given that our only interaction at the quark level is the spin-spin hyperfine term. A more realistic model will require a generalization to include the OGE spin-orbit term and perhaps coupled channel effects, as we discussed in our study of *KN* scattering.

The analytic Born-order result (36) for the phase shifts is unfortunately of little utility for *NN S* waves given realistic quark-model parameters; the equivalent potential $V_{NN}(r)$ is nonperturbatively large in this case, and must be iterated coherently to determine phase shifts, as we have done in Fig. 2 using the *NN* Schrödinger equation. In contrast to this result, we previously found nonperturbative effects in the *S*-wave phase shifts of $\pi\pi$, KK, and KN systems to be much less important, due to somewhat shorter-ranged forces and the smaller reduced mass. The *NN* Born-approximation phase shifts (36) are presumably more useful for higher partial waves and higher energies, since multiple scattering effects are expected to be largest in *S* wave near threshold.

IV. OTHER NONSTRANGE *BB'* CHANNELS: *N*Δ AND ΔΔ

The core potentials predicted by the quark Born formalism for other nonstrange baryon-baryon channels should allow tests of the assumed hyperfine dominance in systems other than the familiar *S*-wave *NN* cases. The short-range interactions in the *N*Δ and ΔΔ channels may be observable experimentally as final-state interactions or, if the interaction is sufficiently strong to support bound states, as dibaryon molecules not far below threshold. The possibility of nonstrange resonances in the q^6 sector has been considered by many authors, the earliest reference apparently being a group-theoretic

TABLE II. Diagram weights for $N\Delta$ elastic scattering.

	ω_1	ω_2	ω_3	ω_4	ω_5	ω_6	ω_7	ω_8
$I=2,\ S=2$	$\frac{7}{9}$	$\frac{1}{9}$	$-\frac{5}{9}$	0	$\frac{2}{9}$	$\frac{2}{9}$	$-\frac{4}{9}$	$-\frac{1}{3}$
$S=1$	$\frac{37}{27}$	$\frac{7}{27}$	$\frac{1}{27}$	$-\frac{4}{27}$	$-\frac{2}{27}$	$-\frac{2}{27}$	$\frac{4}{27}$	$-\frac{1}{27}$
$I=1,\ S=2$	$\frac{13}{27}$	$\frac{7}{27}$	$\frac{1}{27}$	0	$-\frac{2}{27}$	$-\frac{2}{27}$	$\frac{4}{27}$	$\frac{1}{9}$
$S=1$	$\frac{7}{81}$	$\frac{49}{81}$	$-\frac{29}{81}$	$-\frac{28}{81}$	$\frac{2}{81}$	$\frac{2}{81}$	$-\frac{4}{81}$	$\frac{1}{81}$

study by Dyson and Xuong [37]. These q^6 systems have also been studied using the bag model (which is unfortunately known to give unphysical predictions of a host of multiquark resonances), one-boson-exchange models and the nonrelativistic quark model; references before 1985 are summarized by Maltman [33].

Our results for $N\Delta$ and $\Delta\Delta$ are summarized by the diagram weights in Tables II and III. After completing their derivation we found that some of these matrix elements had previously been tabulated by Suzuki and Hecht [35]; our NN and $\Delta\Delta$ weights w_1, w_2, w_3, w_4 are equivalent to the coefficients $C_{ST}^{(5)}, -C_{ST}^{(2)}, -C_{ST}^{(3)}, C_{ST}^{(4)}$ in their Table II, which provides an independent check of our results in these cases. As these weights multiply comparable spatial overlap integrals which give positive contributions to

the low-energy equivalent baryon-baryon potential (34), negative weights imply attractive potential contributions.

Referring to Table II we see that the $N\Delta$ system has a strongly repulsive core in the channels I, S=2,1 and 1,2 and weak core interactions in 2,2 and 1,1. Unlike the $\Delta\Delta$ system (to be discussed subsequently) our $N\Delta$ core interactions do not lead to bound states in any channel. Since the lightest reported dibaryons have masses very close to the $N\Delta$ threshold [36, 38, 39], the experiments may be seeing threshold effects due to the opening of the $N\Delta$ channel, or perhaps weakly bound $N\Delta$ molecules. Our calculation does not support the existence of such bound states, although the NN system is similarly predicted to have a purely repulsive core, but the $I, S = 0, 1$ deuteron is nonetheless bound by an intermediate-range

TABLE III. Diagram weights for $\Delta\Delta$ elastic scattering.

	ω_1	ω_2	ω_3	ω_4	Rel. phase $\omega_5 \ldots \omega_8$
$I=3,\ S=3$	1	-1	-1	1	$(-)$
$S=2$	$\frac{5}{3}$	$-\frac{1}{3}$	$-\frac{1}{3}$	-1	$(+)$
$S=1$	$\frac{19}{9}$	$\frac{1}{9}$	$\frac{1}{9}$	$-\frac{1}{9}$	$(-)$
$S=0$	$\frac{7}{3}$	$\frac{1}{3}$	$\frac{1}{3}$	1	$(+)$
$I=2,\ S=3$	$\frac{1}{3}$	$-\frac{1}{3}$	$-\frac{1}{3}$	$\frac{1}{3}$	$(+)$
$S=2$	$\frac{5}{9}$	$-\frac{1}{9}$	$-\frac{1}{9}$	$-\frac{1}{3}$	$(-)$
$S=1$	$\frac{19}{27}$	$\frac{1}{27}$	$\frac{1}{27}$	$-\frac{1}{27}$	$(+)$
$S=0$	$\frac{7}{9}$	$\frac{1}{9}$	$\frac{1}{9}$	$\frac{1}{3}$	$(-)$
$I=1,\ S=3$	$-\frac{1}{9}$	$\frac{1}{9}$	$\frac{1}{9}$	$-\frac{1}{9}$	$(-)$
$S=2$	$-\frac{5}{27}$	$\frac{1}{27}$	$\frac{1}{27}$	$\frac{1}{9}$	$(+)$
$S=1$	$-\frac{19}{81}$	$-\frac{1}{81}$	$-\frac{1}{81}$	$\frac{1}{81}$	$(-)$
$S=0$	$-\frac{7}{27}$	$-\frac{1}{27}$	$-\frac{1}{27}$	$-\frac{1}{9}$	$(+)$
$I=0,\ S=3$	$-\frac{1}{3}$	$\frac{1}{3}$	$\frac{1}{3}$	$-\frac{1}{3}$	$(+)$
$S=2$	$-\frac{5}{9}$	$\frac{1}{9}$	$\frac{1}{9}$	$\frac{1}{3}$	$(-)$
$S=1$	$-\frac{19}{27}$	$-\frac{1}{27}$	$-\frac{1}{27}$	$\frac{1}{27}$	$(+)$
$S=0$	$-\frac{7}{9}$	$-\frac{1}{9}$	$-\frac{1}{9}$	$-\frac{1}{3}$	$(-)$

attraction which is absent from our leading-order Born calculation. Similar weakly bound states may exist in $N\Delta$ and $\Delta\Delta$ as well, despite repulsive cores.

Next we consider the $\Delta\Delta$ system. For $\Delta\Delta$ some general rules follow from the assumption of a single $\lambda \cdot \lambda$ interaction; since the initial three-quark clusters are transformed into color octets by the interaction, line diagrams with zero or three pairs of quarks exchanged are forbidden. Thus the amplitude for $\Delta^{++}\Delta^-$ elastic scattering must be zero. This implies relations between $\Delta\Delta$ amplitudes with different isospins,

$$h_{fi}(\Delta\Delta; I = 0, S) = -h_{fi}(\Delta\Delta; I = 2, S) \qquad (37)$$

and

$$h_{fi}(\Delta\Delta; I = 1, S) = -\tfrac{1}{9} h_{fi}(\Delta\Delta; I = 3, S) . \qquad (38)$$

Specializing to the $(+)$-symmetry (even-L) cases in Table III, which include the S-wave channels that are *a priori* the most likely to support bound states, it is evident that two $\Delta\Delta$ channels have strongly attractive core potentials, $I, S = 1, 0$ and $0,1$. Of these $0,1$ has the strongest attraction. We search for bound states by solving the Schrödinger equation in the $\Delta\Delta$ system using the low-energy potential (34). With our reference parameter set $\alpha_s/m_q^2 = 5.51$ GeV^{-2} and $\alpha = 0.4$ GeV the attractive core is too weak to induce binding. Note, however, that previous studies of baryons using single Gaussian wave functions have generally assumed a much stronger hyperfine term (see Sec. III). If we use a typical parameter set from these references, $\alpha_s/m_q^2 = 14.9$ GeV^{-2} and $\alpha = 0.32$ GeV (Maltman and Isgur [22]), we find a single S-wave $\Delta\Delta$ bound state in the $0,1$ channel, with $E_B = 40$ MeV. Of course this channel has a fall-apart coupling to NN, so a coupled-channel treatment including the NN system may be required to search for resonant effects. None of the other $\Delta\Delta$ channels have sufficiently strong attractive cores to form bound states in our formalism with the Maltman-Isgur parameters.

Our result for the $I, S = 0, 1$ $\Delta\Delta$ channel is remarkably similar to the conclusion of Maltman [33], who found that the $0,1$ channel has the strongest diagonal attraction in the $\Delta\Delta$ Hilbert space, and that these diagonal forces led to a $\Delta\Delta$ bound state with $E_B = 30$ MeV. Maltman concluded, however, that off-diagonal effects due to the excitation of hidden-color states eliminated this bound state and led to binding in $I, S = 3, 0$ ($E_B = 30$ MeV) and $0,3$ ($E_B = 260$ MeV) instead. The $3,0$ and $0,3$ channels had previously been suggested as possibilities for $\Delta\Delta$ bound states [16, 40, 41]. In contrast we find strong repulsion in the $3,0$ channel and a weak core in $0,3$.

In view of the parameter and approximation dependence of predictions of $\Delta\Delta$ bound states and the theoretical uncertainties in treating hidden-color basis states, the possibility of nonstrange dibaryon molecules should be regarded as an open question for experimental investigation. The channels which appear of greatest interest at present are the attractive-core systems $I, S = 0, 1$ and $1,0$ and the $3,0$ and $0,3$ channels, which previous studies suggested as possibilities for binding.

V. *NN* DIFFERENTIAL CROSS SECTIONS

We can use Eq. (28) of Ref. [27],

$$\frac{d\sigma}{dt} = \frac{4\pi^5 s}{(s - 4M^2)^2} |h_{fi}|^2 , \qquad (39)$$

to determine the nucleon-nucleon differential cross section in leading Born approximation, given the NN h_{fi} matrix element (17). For the experimentally well-determined case of unpolarized PP elastic scattering, we have a weighted sum of the $S = 0$ and $S = 1$ differential cross sections,

$$\left.\frac{d\sigma}{dt}\right|_{PP,\text{unpolarized}} = \frac{1}{4}\left.\frac{d\sigma}{dt}\right|_{I=1,S=0} + \frac{3}{4}\left.\frac{d\sigma}{dt}\right|_{I=1,S=1} . \qquad (40)$$

To obtain the $S = 0$ and $S = 1$ cross sections one simply substitutes the appropriate $I = 1$ diagram weights $\{w_n\}$ from Table I and the integrals $\{I_n\}$ from (29)–(31).

Before we discuss our prediction for this differential cross section we briefly recall the experimental unpolarized PP result. This is shown for a range of P_{lab} in Fig. 3, adapted from Ryan *et al.* [42], Ankenbrandt *et al.* [43], Clyde *et al.* [44], Allaby *et al.* [45], and from the ISR data of Nagy *et al.* [46] and Breakstone *et al.* [47]. The data in the figure were obtained from the Durham-Rutherford HEP data archive. Near threshold the angular distribution is approximately isotropic, but as P_{lab} increases the scattering at large angles falls rapidly, and at high energies the differential cross section is dominated by an asymptotic "diffractive peak,"

$$\lim_{s\to\infty,\ |t|/s\ll 1} \frac{d\sigma}{dt}^{\text{expt}} \approx a e^{bt} . \qquad (41)$$

For the purely hadronic part (as distinct from the divergent forward Coulomb peak) one finds

$$a^{\text{expt}} \approx 70 \text{ mb GeV}^{-2} \qquad (42)$$

and

$$b^{\text{expt}} \approx 11 - 12 \text{ GeV}^{-2} \qquad (43)$$

for the asymptotic form [47].

On evaluating (40) for NN scattering using (17), (39), and Table I we find that several features of the experimental differential cross section at moderate energy are successfully reproduced by our Born-order calculation. The theoretical Born-order cross section (40) which follows from our "reference" parameter set $\alpha_s/m_q^2 = 5.51$ GeV^{-2} and $\alpha = 0.4$ GeV is shown in Fig. 4 for $P_{\text{lab}} = 1.05, 1.75, 3$ and 10 GeV, selected for comparison with Fig. 3. Although $P_{\text{lab}} = 10$ GeV superficially appears to be very relativistic, in the c.m. frame it actually corresponds to $P_{\text{c.m.}} = 2.07$ GeV, which for nucleon-nucleon scattering is only quasirelativistic. As will be discussed below, our quark exchange diagrams are probably irrelevant to diffractive scattering at very high energies.

First note that the smooth evolution from an isotropic angular distribution to an asymptotic forward-peaked one with increasing s is a simple consequence of the suppression in s of all diagrams at small $|t|$ except D_1. In our calculation the contributions of the other diagrams
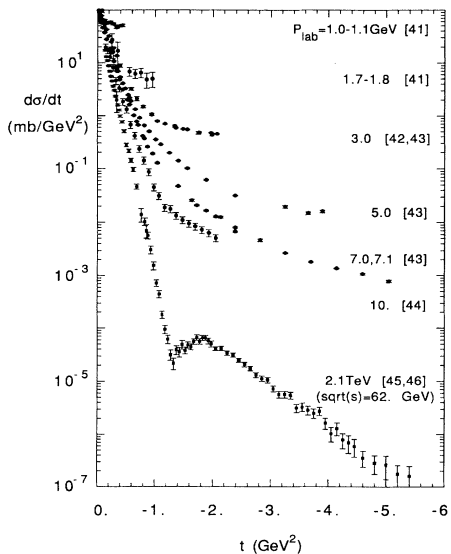
FIG. 3. Unpolarized PP differential cross section. P_{lab} indicated near data sets.

fall exponentially with s. The experimental large-angle scattering does not fall this rapidly, and the discrepancy may be due to our use of single Gaussian forms; the actual proton wave function has short-distance quark-quark correlations, which presumably lead to power-law contributions at large s and $|t|$.

Second, the forward-peaked form of Eq. (41) is predicted by our single Gaussian Born calculation. The overall normalization a and slope parameter b for this process are predicted to be

$$a = \frac{4\pi\alpha_s^2}{9m_q^4}\left(\frac{1}{4}\left(w_1^{I=1,S=0}\right)^2 + \frac{3}{4}\left(w_1^{I=1,S=1}\right)^2\right)$$

$$= \frac{6364}{19683}\frac{\pi\alpha_s^2}{m_q^4} \tag{44}$$

and

$$b = \frac{2}{3\alpha^2} . \tag{45}$$

The theoretical result (44) for the magnitude of the forward peak is actually independent of the spatial wave function, since the defining integral (23) is just the product of two normalization integrals in the limit $\mathbf{A} = \mathbf{C}$.

With our reference parameter set we predict a somewhat smaller, broader peak than is observed experimentally at high energy, with

$$a = 12 \text{ mb GeV}^{-2} \tag{46}$$

and

$$b = 4.2 \text{ GeV}^{-2} . \tag{47}$$

Both a and b, however, are sensitive to the choice of quark model parameters, and vary by factors of about 10 and 3, respectively, when α_s/m_q^2 and α are varied through a plausible range, which we shall discuss below.
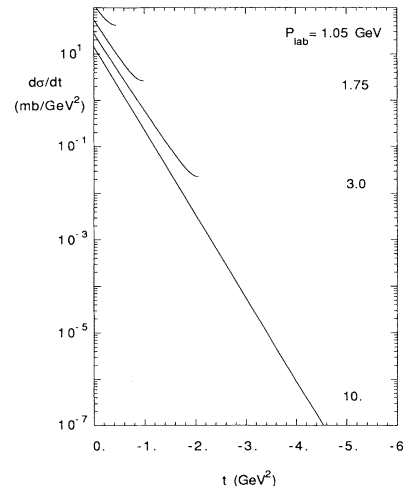

FIG. 4. Theoretical unpolarized PP differential cross section. Parameter set $\alpha_s m_q^2 = 0.6/(0.33)^2$ GeV^{-2} and $\alpha = 0.4$ GeV.

If we use typical intercept and slope values of $a = 70$ mb GeV^{-2} and $b = 11$ GeV^{-2} as input to fix our two parameters we obtain

$$\frac{\alpha_s}{m_q^2} = 13.3 \text{ GeV}^{-2} \tag{48}$$

corresponding to $m_q = 0.21$ GeV if we leave $\alpha_s = 0.6$, and

$$\alpha = 0.246 \text{ GeV} \tag{49}$$

which are in the range of the values discussed in Sec. III.

Although we can fit the magnitude and t dependence of the small-$|t|$ differential cross section at high energies reasonably well with our quark Born results, we emphasize that this is not a realistic description of diffractive scattering. The Born amplitude is purely real whereas the experimental small-$|t|$ amplitude is known to be close to imaginary [46, 48]. This implies that the first Born approximation is inadequate for small-$|t|$ diffractive scattering, and that the coupling to inelastic channels is an essential component of a description of the diffractive amplitude, even for elastic processes [49]. Another argument against this mechanism is the similarity of pp and $p\bar{p}$ scattering at very high energy which argues in favor of multigluon exchange diagrams as the origin of diffractive scattering. Such processes appear at higher order in the Born series. Thus it would be interesting to iterate diagram D_1 [50] to examine the possibility that this simple model may explain the observed t dependence of the diffractive peak.

VI. SUMMARY AND CONCLUSIONS

We have applied the quark-Born-diagram formalism to nonstrange baryon-baryon elastic scattering. In this ap-

proach the hadron-hadron scattering amplitude is taken to be the sum of all single quark-pair interactions followed by all allowed quark interchanges, with nonrelativistic quark model wave functions attached to the external lines. This may be a useful description of reactions which are free of $q\bar{q}$ annihilation. The model has few parameters (here only two, the baryon oscillator parameter α and the hyperfine strength α_s/m_q^2, since we incorporate only the OGE spin-spin hyperfine term in this study), and with Gaussian wave functions and a contact interaction the scattering amplitudes can be derived analytically. The model was previously applied to $I = 2$ $\pi\pi$ and $I = 3/2$ $K\pi$ scattering with good results, and also gives reasonable results for low-energy S-wave KN scattering, although there are discrepancies at higher energies and in higher partial waves.

NN scattering is an important test of this approach because it is also annihilation free (at the valence quark level), and the baryon wave function and the dominance of the spin-spin OGE hyperfine interaction in *NN* are already reasonably well established. We find that the quark Born diagrams predict repulsive core interactions in both S-wave *NN* channels, and the equivalent low-energy potentials we extract from the scattering amplitudes are very similar to the results of previous resonating-group and variational calculations. In view of the complexity of the baryon-baryon scattering problem, which involves a sum of thousands of diagrams and the evaluation of 36-dimensional overlap integrals, we find our approximate agreement with experiment encouraging.

We also give results for the $N\Delta$ and $\Delta\Delta$ core interactions induced by the OGE spin-spin term, and find that certain $\Delta\Delta$ channels have attractive cores and may possess bound states. Finally we determine the *NN* differential cross section predicted by our Born amplitude, and compare the results with the experimental unpolarized PP differential cross section. We find that several well-known features of experimental PP scattering at intermediate energies are evident in our Born results, including the development of a forward peak with a qualitatively correct width and magnitude.

ACKNOWLEDGMENTS

APPENDIX: DISCUSSION OF NUCLEON WAVE-FUNCTION PARAMETERS

Examples of previous values of α_s/m_q^2 (in chronological order) are $\alpha_s/m_q^2 = 15.5$ GeV^{-2} (Oka and Yazaki, 1980 [16]); 37.8 GeV^{-2} (Harvey, 1981 [12]; this value now appears exceptionally large); 7.7 GeV^{-2} (Faessler *et al.*, 1982 [13]); 14.9 GeV^{-2} (Maltman and Isgur, 1984 [22]); and 14.4 GeV^{-2} (Koike, 1986 [18]). Large values were required to fit the N-Δ mass splitting given single Gaussian wave functions; since this is proportional to $(\alpha_s/m_q^2)|\psi(0)|^2$, an underestimated wave function at contact must be compensated for by a large (α_s/m_q^2). If one instead uses the actual Coulomb plus linear wave functions from the nonrelativistic Schrödinger equation with $m_q \approx 0.3$ GeV, the larger value of $|\psi(0)|$ leads to a much smaller $\alpha_s/m_q^2 \approx 5$ GeV^{-2}. Since our scattering calculation uses Gaussian wave functions one could argue which parameter value is most appropriate; an improved calculation with more realistic wave functions will probably be required to eliminate these parameter uncertainties.

The baryon width parameter α has also been assigned a rather large range of values in previous work. Representative values in chronological order are $\alpha = 0.41$ GeV (Copley, Karl, and Obryk, baryon photocouplings, 1969 [51]); 0.32 GeV (Isgur and Karl, baryon spectroscopy, 1979 [52]); 0.41 GeV (Koniuk and Isgur, baryon photocouplings, 1980 [53]); 0.33 GeV (Oka and Yazaki, *NN* interactions, 1980 [16]); 0.25 GeV (Harvey, *NN* interactions, 1981 [12]); 0.42 GeV (Faessler *et al.*, *NN* interactions, 1982 [13]); 0.25 GeV (Hayne and Isgur relativized quark model, 1982 [54]); 0.32 GeV (Maltman and Isgur, *NN* interactions, 1984 [22]); 0.34 GeV (Koike, *NN* interactions, 1986 [18]); 0.3 and 0.42 GeV, with the smaller value preferred (Li and Close, baryon electroproduction, 1990 [55]).

Most potential models assume a value of m_q near 0.3 GeV, although the relativized models of Hayne and Isgur [54], Godfrey and Isgur (mesons) [56], and Capstick and Isgur (baryons) [57] use a lower value of 0.22 GeV. Although these relativized models also use a small value of $\alpha_s(Q^2 = 0) = 0.6$ for the infrared limit of an effective running $\alpha_s(Q^2)$, the hyperfine strength $\alpha_s(0)/m_q^2 = 12.2$ GeV^{-2} is again large because of the smaller m_q. Its effects are reduced, however, by the use of a "smeared" contact interaction.

We note that the smaller value of α_s we use is now generally preferred because recent spectroscopy studies using improved wave functions have considerably lowered the value required to fit hadron spectroscopy. The *NN* references we compare with predate the improved spectroscopy studies and thus used a rather large value of α_s, which was required to give a realistic $N\Delta$ splitting given single Gaussian wave functions. We also prefer to use our fixed parameter set because these values were found to give reasonable results for low-energy S-wave $\pi\pi$, $K\pi$, and KN scattering in our previous studies [27, 28, 32].

[1] P.M. Morse, J.B. Fisk, and L.I. Schiff, Phys. Rev. **50**, 748 (1936); H.A. Bethe and R.F. Bacher, Rev. Mod. Phys. **8**, 82 (1936), acknowledge the possibility of a potential of this general form but were skeptical, see especially Sec. 27, p. 161; subsequent early references include G. Parzen and L.I. Schiff, Phys. Rev. **74**, 1564 (1948); R. Jastrow, *ibid.* **79**, 389 (1950), and references cited therein; *ibid.*, **81**, 165 (1951).

[2] H. Yukawa, Proc. Phys. Math. Soc. Jpn. **17**, 48 (1935).

[3] See, for example, M. Lacombe, B. Loiseau, J.M. Richard, and R. VinhMau, Phys. Rev. C **21**, 861 (1980); K. Holinde, Phys. Lett. **68C**, 121 (1981); R. Machleidt, Adv. Nucl. Phys. **19**, 189 (1989); E. Hummel and J.A. Tjon, Phys. Rev. C **42**, 423 (1990); F. Gross, J.W. VanOrden, and K. Holinde, *ibid.* **45**, 2094 (1992).

[4] N. Isgur, Acta Phys. Austriaca, Suppl. **XXVII**, 177 (1985).

[5] P.J. Siemens and A.S. Jensen, *Elements of Nuclei; Many-Body Physics with the Strong Interaction*, Sec. 2.6 (Addison-Wesley, New York, 1987).

[6] C.E. DeTar, Phys. Rev. D **17**, 302 (1977); **17**, 323 (1977); Prog. Theor. Phys. **66**, 556 (1981); **66**, 572 (1981).

[7] Y. Nambu, in *Preludes in Theoretical Physics*, edited by A. deShalit, H. Feshbach, and L. vanHove (North-Holland, Amsterdam, 1966).

[8] A. De Rújula, H. Georgi, and S.L. Glashow, Phys. Rev. D **12**, 147 (1975).

[9] H.J. Schnitzer, Phys. Rev. Lett. **35**, 1540 (1975).

[10] D.A. Liberman, Phys. Rev. D **16**, 1542 (1977).

[11] V.G. Neudatchin, Y.F. Smirnov, and R. Tamagaki, Prog. Theor. Phys. **58**, 1072 (1977); I.T. Obukhovsky, V.G. Neudatchin, Y.F. Smirnov, and Y.M. Tchuvil'sky, Phys. Lett. **88B**, 231 (1979).

[12] M. Harvey, Nucl. Phys. **A352**, 326 (1981).

[13] A. Faessler, F. Fernandez, G. Lübeck, and K. Shimizu, Nucl. Phys. **A402**, 555 (1983).

[14] M. Harvey, J. Letourneaux, and B. Lorazo, Nucl. Phys. **A424**, 428 (1984).

[15] C.S. Warke and R. Shanker, Phys. Rev. C **21**, 2643 (1980).

[16] M. Oka and K. Yazaki, Phys. Lett. **90B**, 41 (1980).

[17] J.E.T. Ribeiro, Z. Phys. C **5**, 27 (1980).

[18] Y. Koike, Nucl. Phys. **A454**, 509 (1986).

[19] K. Yazaki, Nucl. Phys. **A416**, 87c (1984); M. Oka and C.J. Horowitz, Phys. Rev. D **31**, 2773 (1985); F. Lenz, J.T. Londergan, E.J. Moniz, R. Rosenfelder, M. Stingl, and K. Yazaki, Ann. Phys. (N.Y.) **170**, 65 (1986); Yu.A. Kuperin, S.B. Levin, and Yu.B. Melnikov, "Generalized String-Flip Model for Quantum Cluster Scattering," Department of Mathematics and Computational Physics, St. Petersburg University report, Sec. 5 (1992).

[20] Z.-J. Cao and L.S. Kisslinger, Phys. Rev. C **40**, 1722 (1989).

[21] K. Shimizu, Rep. Prog. Phys. **52**, 1 (1989).

[22] K. Maltman and N. Isgur, Phys. Rev. D **29**, 952 (1984).

[23] T. Goldman, G.J. Stephenson, K. Maltman, and K.E. Schmidt, Nucl. Phys. **A481**, 621 (1988); T. Goldman, K. Maltman, G.J. Stephenson, K.E. Schmidt, and Fan Wang, Phys. Rev. C **39**, 1889 (1989); Fan Wang, Guang-Han Wu, Li-Jian Teng, and T. Goldman, Phys. Rev. Lett. **69**, 2901 (1992).

[24] See, for example, J.F. Gunion, S.J. Brodsky, and R. Blankenbecler, Phys. Rev. D **8**, 287 (1973); S.J. Brod-

sky and G.R. Farrar, *ibid.* **11**, 1309 (1975); G.P. Lepage and S.J. Brodsky, *ibid.* **22**, 2157 (1980); G. Farrar, Phys. Rev. Lett. **53**, 28 (1984); S.J. Brodsky and G.P. Lepage, in *Perturbative Quantum Chromodynamics*, edited by A. Muller (World Scientific, Singapore, 1989).

[25] J. Botts and G. Sterman, Nucl. Phys. **B325**, 62 (1989); J. Botts, *ibid.* **B353**, 20 (1991).

[26] N. Isgur and C.H. Llewellyn Smith, Phys. Lett. **B217**, 535 (1989).

[27] T. Barnes and E.S. Swanson, Phys. Rev. D **46**, 131 (1992).

[28] T. Barnes, E.S. Swanson, and J. Weinstein, Phys. Rev. D **46**, 4868 (1992).

[29] See, for example, D. Blaschke and G. Röpke, Phys. Lett. **B299**, 332 (1993); J. Weinstein and N. Isgur, Phys. Rev. D **41**, 2236 (1990); B. Masud, J. Paton, A.M. Green, and G.Q. Liu, Nucl. Phys. **A528**, 477 (1991); and references cited therein.

[30] E.S. Swanson, Ann. Phys. (N.Y.) **220**, 73 (1992).

[31] K. Dooley, E.S. Swanson, and T. Barnes, Phys. Lett. B **275**, 478 (1992); K. Dooley, University of Toronto, Ph.D. thesis (1993); G. Karl, "Exotica, Survey of Exotic Mesons," in Proceedings of the Second Biennial Conference on Low Energy Antiproton Physics "LEAP '92" (Courmayeur, Italy, 14-19 September 1992).

[32] T. Barnes and E.S. Swanson, MIT/ORNL report MIT-CTP-2169, ORNL-CCIP-92-15, 1992 (unpublished).

[33] K. Maltman, Nucl. Phys. **A438**, 669 (1985).

[34] F. Gross (private communication).

[35] Y. Suzuki and K.T. Hecht, Phys. Rev. C **27**, 299 (1983).

[36] R.A. Arndt, L.D. Roper, R.L. Workman, and M.W. Mc-Naughton, Phys. Rev. D **45**, 3995 (1992).

[37] F.J. Dyson and N.-H. Xuong, Phys. Rev. Lett. **13**, 815 (1964).

[38] M.P. Locher, M.E. Sainio, and A. Svarc, Adv. Nucl. Phys. **17**, 47 (1986); K.K. Seth, in *Proceedings of the Third Workshop on Perspectives in Nuclear Physics at Intermediate Energies*, Trieste, 1987, edited by S. Boffi *et al.* (World Scientific, Singapore), pp. 37–68.

[39] M. Aguilar-Benitez *et al.*, Phys. Lett. **170B**, 1 (1986).

[40] T. Kamae and T. Fujita, Phys. Rev. Lett. **38**, 471 (1977).

[41] M. Cvetič, B. Golli, N. Mankoč-Borštnik, and M. Rosina, Phys. Lett. **93B**, 489 (1980).

[42] B.A. Ryan *et al.*, Phys. Rev. D **3**, 1 (1971).

[43] C.M. Ankenbrandt *et al.*, Phys. Rev. **170**, 1223 (1968).

[44] A.R. Clyde *et al.*, Report No. UCRL-16275, 1966 (unpublished).

[45] J.V. Allaby *et al.*, Nucl. Phys. **B52**, 316 (1973).

[46] E. Nagy *et al.*, Nucl. Phys. **B150**, 221 (1979).

[47] A. Breakstone *et al.*, Phys. Rev. Lett. **54**, 2180 (1985).

[48] UA4 Collaboration, D. Bernard *et al.*, Phys. Lett. B **198**, 583 (1987); P.V. Landshoff, CERN Report No. CERN-TH.6277/91.

[49] R.J.N. Phillips (private communication).

[50] R.G. Roberts (private communication).

[51] L.A. Copley, G. Karl, and E. Obryk, Nucl. Phys. **B13**, 303 (1969).

[52] N. Isgur and G. Karl, Phys. Rev. D **20**, 1191 (1979).

[53] R. Koniuk and N. Isgur, Phys. Rev. D **21**, 1868 (1980).

[54] C. Hayne and N. Isgur, Phys. Rev. D **25**, 1944 (1982).

[55] Z. Li and F.E. Close, Phys. Rev. D **42**, 2207 (1990).

[56] S. Godfrey and N. Isgur, Phys. Rev. D **32**, 189 (1985).

[57] S. Capstick and N. Isgur, Phys. Rev. D **34**, 2809 (1986).